

This manuscript has been submitted to the
Canadian Journal of Civil Engineering
to provide information before publication.
The contents are subject to change.

**INITIAL FRACTURE AND BREAKUP
OF RIVER ICE COVER**

by

S. Beltaos

**Rivers Research Branch
National Water Research Institute
Canada Centre for Inland Waters
Burlington, Ontario, L7R 4A6**

**February 1989
NWRI Contribution #89-70**

ABSTRACT

When runoff begins, uplift pressures develop on the underside of the shore fast cover. Analysis shows that longitudinal cracks should form soon after runoff starts. Two cracks are normally predicted, subdividing the cover into a main central part and two side strips. Where ice thickness is large or the channel narrow, a single mid-channel crack is predicted. Field observations support the theory.

With increasing flow, the central portion of the cover may detach and become subject to transverse fractures. The latter could result from bending on vertical or horizontal planes. Vertical bending fracture requires extreme, wave-like slopes such as might prevail briefly during jam releases. Flow shear and the meandering planform of rivers cause horizontal bending which is favoured by observed transverse crack patterns. The resulting separate ice sheets will be set in motion if there is enough room on the water surface between the river boundaries, thus initiating the breakup. The attendant forecasting criterion, called the boundary constraint, explains past empirical findings and identifies the factors influencing various empirical coefficients.

Another type of breakup is caused by ice-jam releases and formation of breaking fronts whereby the ice cover is reduced to rubble before it moves. Little is known about the motion of breaking fronts but relevant field observations are reviewed.

RÉSUMÉ

Quand l'écoulement des eaux de fonte commence, des pressions croissantes exercées vers le haut apparaissent sous la couverture de glace de rive. L'analyse indique que des fissures longitudinales devraient se former peu après le début de cette période. On prévoit normalement la formation de fissures, subdivisant la couverture en une partie centrale principale et en deux bandes latérales. Quand l'épaisseur de la glace est élevée ou que les canaux sont étroits, on prévoit la formation d'une seule fissure au milieu du canal. Les observations sur place confirment cette théorie.

Quand l'écoulement devient plus important, la partie centrale de la couverture peut se détacher et être soumise à diverses fractures transversales. Ces dernières peuvent résulter de la flexion des glaces selon des plans verticaux ou horizontaux. Les fractures dues aux flexions verticales nécessitent des pentes de type ondulé comme on peut en observer pendant de brefs intervalles lors de la rupture des embâcles. Le cisaillement dû à l'écoulement et les méandres du plan des rivières sont à l'origine de flexions horizontales, indiquées par l'observation de motifs formés de fissures transversales. Les plaques de glace qui en résultent seront mises en mouvement s'il y a suffisamment de place à la surface de l'eau entre les rives du cours d'eau, ce qui entraînera leur bris. Les critères de prévision de cette théorie, appelés contraintes dues aux limites, expliquent des observations empiriques antérieures et identifient les facteurs influençant divers coefficients empiriques.

Un autre type de bris est causé par les débâcles et la formation de fronts de dislocation dans lesquels la couverture de glace est réduite en fragments avant d'avoir pu se déplacer. On connaît très peu de choses sur les mouvements qui surviennent dans ces fronts, mais on étudie présentement les observations sur place pertinentes.

MANAGEMENT PERSPECTIVE

River ice breakup is often attended by destructive ice jams that cause flooding and other damages. While considerable progress has been made in predicting features of jams once they have formed, little is known about the processes by which the continuous winter ice cover is fractured and eventually reduced to small ice blocks that form ice jams. Understanding these processes is essential to forecasting the onset and severity of breakup, an important component of river ice management.

In this paper, various mechanisms involved in the breakup process are described and quantified by means of analysis and field data. Generalized breakup forecasting criteria are obtained as a result and the governing hydro-thermal and mechanical factors identified.

PERSPECTIVE-GESTION

Lors de la rupture de la couverture de glace des cours d'eau, il y a souvent formation d'embâcles destructeurs qui sont à l'origine d'inondations et d'autres dommages. Bien que des progrès considérables aient été réalisés dans la prévision des caractéristiques des embâcles déjà formés, on ne connaît que peu de choses sur les processus responsables de la fracturation de la couverture de glace continue d'hiver et de sa dislocation éventuelle en petits blocs de glace qui forment les embâcles. La compréhension de ces processus est essentielle pour la prévision du début et de l'importance du bris, ce qui constitue un élément important de la gestion des glaces des cours d'eau.

Dans ce document, les divers mécanismes responsables du processus de bris sont décrits et identifiés par des analyses et des données d'observation sur place. Cette étude a permis d'obtenir des critères généraux de prévision de la rupture ainsi que d'identifier les facteurs mécaniques et hydrothermiques qui les régissent.

INTRODUCTION

The breakup of river ice is a brief but important period of the year because of the frequent formation of destructive ice jams. While considerable progress has been made in predicting features of ice jams once they are in place, little is known about the processes by which the continuous winter ice cover is fractured into the small fragments that comprise an ice jam. Understanding these processes is essential to forecasting both the onset and the severity of the breakup.

Two common occurrences of the initial phases of breakup are analysed herein, the formation of longitudinal and transverse cracks. In this manner, the initially continuous ice cover breaks down into separate sheets which often sets the stage for breakup "initiation", if this event is defined as the time when the cover is set in motion. Once this occurs, further fragmentation is rapid via impacts of moving ice sheets either on channel boundaries or on other ice sheets. The initial pattern of fracture governs the sizes of the separate ice sheets which in turn may influence the conditions for breakup initiation and, later, on the location and persistence of ice jams. It is shown that this concept can be used to develop forecasting criteria and explain some of the empirical findings to date.

A more immediate type of ice breaking occurs during surges that follow the releases of major jams. Here the ice cover can be reduced to rubble very rapidly and, often, before it is even set in motion. This phenomenon is not quantifiable at present owing to lack of detailed field and laboratory data.

LONGITUDINAL CRACKS

Physical Considerations and Assumptions

Consider the case of an ice-covered river reach, in which steady uniform flow prevails, as is approximately the case during the winter period. The flow under the cover can be described as gravity-driven with nearly hydrostatic pressure distribution.

When warm weather and increased runoff start, the discharge will begin to increase with time and upstream distance. So long as the cover remains integral and attached to the river banks, a pressure gradient must develop to accommodate the increased discharge. The flow will thus become of the conduit type and be partly pressure-driven. Increasing uplift pressures will be applied to the ice cover until the latter's strength is exceeded and cracks form. Once this occurs, the water will be free to assume a higher stage and revert to purely gravity-driven flow while the cracked cover will float to a higher position.

Prior to crack formation, the structural situation is that of a floating ice plate, supported at the edges and subjected to a distributed load, p , as illustrated in Figure 1. Considering the total upward pressure, p_T , applied on the underside of the ice cover at its deformed state, we obtain:

$$[1] \quad p_T = p + \gamma(s_i h_i - w) - \gamma_i h_i$$

in which γ , γ_i = unit weights of water and ice, respectively; h_i = ice cover thickness; w = deflection of the ice cover; and $s_i = \gamma_i/\gamma$ = specific gravity of ice = 0.92. Eq. 1 can be simplified to

$$[2] \quad p_T = p - \gamma w$$

which suggests that the ice cover may be assumed to behave as a plate subjected to an upward distributed load, p , and supported from above by an elastic foundation¹ of modulus equal to γ . Eqs. 1 and 2 are valid so long as the bottom of the ice cover does not emerge above the water level, i.e., $w \leq s_i h_i$. This condition is usually satisfied in practice and will be assumed to apply herein. The load p is laterally uniform but must vary

¹An elastic foundation produces a reaction that is proportional to the local deflection. The coefficient of proportionality is called the foundation modulus.

with longitudinal distance and time in view of the unsteady flow conditions that prevail when the discharge starts to increase. The actual situation is thus too complex for analytical solution but can be considerably simplified by making the following two assumptions: (a) dynamic effects are negligible; and (b) the longitudinal gradient of p is small. These assumptions can be verified by an order-of-magnitude analysis (Beltaos 1985). The solution can thus be based on the theory of beams resting on elastic foundations (Hetenyi 1946). A solution for infinitely long beams (very wide channel) has already been obtained by Billfalk (1981).

Analytical Relationships

For a beam of arbitrary length, Hetenyi (1946) gives the following expressions for the bending moment:

$$[3] \quad \frac{2\lambda^2 M}{p} = \frac{\sinh \lambda z \sin \lambda z^1 + \sinh \lambda z^1 \sin \lambda z}{\cosh \lambda W + \cos \lambda W} ; \text{ hinged ends}$$

$$[4] \quad \frac{2\lambda^2 M}{p} = \frac{1}{\sinh \lambda W + \sin \lambda W} (\sinh \lambda z \cos \lambda z^1 + \cos \lambda z \sinh \lambda z^1 - \sin \lambda z \cosh \lambda z^1 - \cosh \lambda z \sin \lambda z^1); \text{ fixed ends}$$

in which M = bending moment per unit width; p = uniformly distributed load per unit width applied on the beam; z = distance from the left ice edge; z^1 = distance from the right ice edge = $W - z$; W = ice cover width; and λ is defined by

$$[5] \quad \lambda = \sqrt[4]{\gamma/4EI}$$

in which E = elastic modulus of ice; and I = moment of inertia of ice cover per unit width = $h_i^3/12$. Substituting in [5] and re-arranging gives the more convenient, dimensionless expression:

$$[6] \quad \lambda h_i = \sqrt[4]{3\gamma h_i/E}$$

Eqs. 3 and 4 may be used to study the location of maximum M and the uplift pressure necessary to cause cracking of the cover. First, the case $\lambda W \rightarrow \infty$ is considered. Eqs. 3 and 4 reduce to

$$[7] \quad \frac{2\lambda^2 M}{p} = e^{-\lambda z} \sin \lambda z; \text{ hinged ends}$$

$$[8] \quad \frac{2\lambda^2 M}{p} = e^{-\lambda z} (\sin \lambda z - \cos \lambda z); \text{ fixed ends}$$

These expressions are identical to Billfalk's (1981) for the infinitely wide channel case.

For finite channel widths, [3] and [4], along with corresponding equations for ice deflection (Hetenyi 1946) can be used to determine moment and deflection variations across the channel. Typical results for hinged ends are shown in Figures 2 and 3. Figure 2 shows that maximum bending occurs at mid-stream for $\lambda W \leq 3.0$ which suggests that only one central crack should

form in this case. However, as λW increases above 3, the maximum bending moments are no longer located at mid-stream which implies that two longitudinal cracks should form, each located a distance l_s off the respective channel end. For the case of fixed ends the calculations have indicated that $l_s = 0$, i.e., maximum bending occurs at the channel edges.

Figure 4 shows the variation of l_s/W with λW and Figure 5 gives the uplift pressure required to cause crack formation, $p_f (= \gamma \Delta H)$, as a function of λW as well as ice thickness and ice properties (note that $\sigma_1 =$ flexural strength of the ice cover). Figures 4 and 5 indicate that an ice cover may be considered "infinitely" wide if $\lambda W \geq 6$.

The present results also apply to the case of an ice cover subjected to a drop in the water level, provided the bottom of the cover is everywhere in contact with water. This property was utilized by Billfalk (1981) to test his analysis and obtain good agreement with observation, using $E = 6.5$ GPa. The latter figure is practically the same as 6.8 GPa, recommended by Gold (1971) for good-quality freshwater ice.

Where cracking is the result of uplift pressures, as happens near the time of breakup, it is not possible to know before hand whether the end supports are fixed or hinged. However, when longitudinal cracks are offset, i.e., they are located some distance off the edges ("hinge" cracks), one could assume hinged supports. Where no cracks are present, even

though the ice cover is detached from the river banks, one must assume that either the end supports were fixed, or the adhesion of the ice to the banks was too low to permit development of hinge cracks. In the writer's experience, longitudinal cracks are usually offset so that the hinged support type would seem to be a common occurrence.

From observations of crack locations in the Thames River (Ontario), a value of $E = 1.4$ GPa has been deduced. This is about five times less than the elastic modulus of good-quality ice subjected to rapid loading. The difference is large but can be attributed to creep effects, as shown by Beïtaos (1985).

Case Studies and Examples

Using $E = 1.4$ GPa, we now proceed to describe a few field observations and compare them to prediction.

- (1) Thames River at Thamesville, 1981 and 1982. Observed $l_s = 5.0$ m; $h_f = 0.32$ m; $W = 40$ m. From Eq. 5 we find $\lambda = 0.16$ m⁻¹ and $\lambda W = 6.4$ which exceeds 6.0 so that the infinite-width formulae apply. It follows that the predicted value of l_s is equal to $\pi/4\lambda$ (see [7]), i.e., $l_s = 4.9$ m which is close to the observed value.

- (2) Thames River near Louisville, 1983. Observed $l_s = 2.0$ m; $h_i = 0.11$ m; $W = 55$ m. We find $\lambda = 0.35$ m⁻¹ and $\lambda W = 19.5$. Therefore, predicted $l_s = \pi/4\lambda = 2.2$ m which is close to the observed value.
- (3) For several Manitoba streams, it has been observed that a single central crack occurs for widths less than 30 m (J. Wedel, personal communication). Figure 4 then implies that λW should be less than 3.0. Therefore λ should not exceed $3/30 = 0.1$ m⁻¹. Using [5] gives $h_i > 0.6$ m which was indeed the case for the streams under consideration (J. Weddel, personal communication).
- (4) Grand River near Leggatt, 1982. A single, mid-channel crack was observed in this reach prior to breakup. Accurate values of h_i and W are not available. Ice thickness has been estimated as 0.45 m from measurements elsewhere on the Grand River. The channel width has been assumed to be 27 m, a value measured under open water conditions at a stage similar to that which prevailed when the crack was observed. Putting $E = 1.4$ GPa and $h_i = 0.45$ m in [5] gives $\lambda = 0.12$ m⁻¹ and $\lambda W = 3.3$ which, from Figure 4, suggests that two cracks should form, contrary to what was observed. However, the accuracy of h_i and W is such that λW

could easily have been 3 or less which would indicate only one crack formed. Moreover, inspection of Figure 2 indicates that when λW is between 3 and 3.5, the maximum bending moment is only slightly more than the central moment. If, as is often the case, h_i varies somewhat across the stream, being thinner near the centre, a central crack would form even if $\lambda W > 3$ (note that bending stress varies as $1/h_i^2$).

As an example of applying the present results, let $h_i = 0.50$ m, $W = 50$ m, $E = 1.4$ GPa and $\sigma_i = 600$ kPa; then [5] gives

$$\lambda = \{9.81 \times 10^3 / (4 \times 1.4 \times 10^9 \times 0.5^3 / 12)\}^{1/4} = 0.11 \text{ m}^{-1}$$

Hence $\lambda W = 5.7$ and $\lambda h_i = 0.057$. From Figure 5 we find that $p_f / \sigma_i (\lambda h_i)^2 = 1.04$, hence $p_f = 2.0$ kPa. After formation of cracks, the middle strip of the ice cover would float to an elevation exceeding the pre-stressing elevation by $\Delta H (= 2.0 \times 10^3 / 9.8 \times 10^3) = 0.21$ m. Figure 3 indicates that the maximum deflection is about $1.1 p_f / \gamma = 1.1 \times 0.21 = 0.23$ m which is less than $s_i h_i (= 0.92 \times 0.5 = 0.46$ m), as is required for the theory to apply. For $\lambda W = 5.7$, Figure 4 gives $l_s / W = 0.14$ and $l_s = 6.9$ m. Beltaos (1985) showed that only a small increment in discharge is needed to cause longitudinal

cracks which suggests that they should form shortly after runoff begins. However, full separation of the resulting ice strips does not become evident until a significant rise in the water level and river width occurs.

The preceding examples show that the simple analysis presented herein accounts for the main mechanisms involved. At the same time, one should keep in mind various complications that may arise from the irregularity of natural streams. For example, trees or boulders on the river banks may become "anchor" points when the ice cover forms and change the edge support configuration from a continuous one to that of a series of irregularly spaced point supports. As the river level drops in early winter, several longitudinal cracks may form near each edge due to freezing of the shallow water near the banks; the cracks usually freeze over but their presence may influence the location of uplift cracking during runoff events.

TRANSVERSE CRACKS - "HORIZONTAL" BENDING

Transverse cracks are often observed before the breakup starts. The mechanisms responsible for transverse cracking can be investigated by examining the spacing of the cracks and the stresses required to produce them.

Plausibility of Horizontal Bending

Shulyakovski (1972) proposed that transverse cracking occurs by stressing on planes parallel to the water surface (herein called, with some license, horizontal planes for simplicity). This mechanism is illustrated in Figure 6 where it is shown that bending stresses develop in the ice cover via the accumulated effects of the flow shear stress and the downslope component of the weight of the cover². In a straight river, only compressive stresses can develop by these forces (excepting the slight bending due to the eccentricity of the flow shear) but, in a meandering one, bending moments and attendant tensile stresses are also present. It will be shown later that such stresses can cause transverse cracks spaced relatively far apart (order of a thousand ice thicknesses). This is consistent with observations. For example, Nuttall (1970) observed spacings of ~4-5 river widths in the N. Saskatchewan and Pembina Rivers which translates to 700-1,500 h_i . Transverse crack spacings, averaging 1,000-1,600 h_i have been observed by the writer in the Thames River during the 1982 and 1984 breakup events. The 1982 results have already been reported (Beltaos 1984a). In 1984, two breakups occurred, the first in February and the

²Figure 6 is a more general version of Shulyakovski's concept that assumed the river to consist of a sequence of linear segments.

second in March. The March ice cover was relatively thin owing to the brevity of the cold period between the two events. Statistical distributions of l_i (= distance between consecutive cracks) are plotted in Figure 7 where they appear to be approximately log-normal.

The Thames River data are detailed enough to enable a rough check on the plausibility of the horizontal bending concept. A major uncertainty pertains to the forces transferred between adjacent ice sheets following formation of a crack and just before formation of the next one downstream. With reference to Figure 8, a range can be defined, however, by considering the two limiting cases of (a) no force is transferred, and (b) the full force (but no moment) is transmitted from sheet AB to sheet BC. Contributions from sheets further upstream are neglected.

It can be shown (Beltaos 1984a) that the bending moment M at C is (Figure 8):

$$[8] \quad M = 2\tau W_i (a \text{ or } A)$$

in which W_i = width of ice cover; a , A = areas defined in Figure 8, corresponding to cases (a) and (b) above; and $\tau = \tau_i + s_i \gamma h_i S$, with τ_i = flow shear stress applied on the ice cover and S = water surface slope. When M becomes equal to $\sigma_i h_i W_i^2 / 6$, a transverse crack should form, and from [8], we obtain:

$$[9] \quad \sigma_i = 12 \tau (a \text{ or } A)/h_i W_i$$

Table 1 summarizes characteristics of the ice sheets observed in the Thames River, including estimates of σ_i via [9]. These values seem very low relative to 400-600 kPa, an "expected" range of flexural strength for competent pre-breakup ice, based on conventional small-scale testing (e.g., Korzhavin 1971; Butyagin 1972). The discrepancy can be explained by the well-known, though not as well understood, tendency of ice to appear weaker as specimen thickness (corresponding to ice cover width for horizontal bending) increases. Note that the σ_i 's in Table 1 refer to the entire ice cover and see details and pertinent test data in Appendix A. It is thus concluded that horizontal bending can account for far-spaced transverse cracks.

Size of Ice Sheets

The length of ice sheets produced by transverse fracture is an important parameter because of its possible influence on the breakup process (see also later discussion). A major difficulty in predicting this length derives from the uncertainty as to the actual bending moment responsible for fracture (see Eq. 8). If we assume, for simplicity, that geometric similarity exists among the planforms of various river reaches, both a and A would vary in proportion to l_i^2 (l_i = length of an ice sheet).

This is confirmed in Figure 9 where the Thames River data are plotted together with pertinent information from the Mackenzie River (Anderson 1982). It follows that the bending moment, M , varies in proportion to $\tau W_i l_i^2$ (Eq. 8) and, since the resistance to bending is proportional to $\sigma_i h_i W_i^2$:

$$[10] \quad l_i = \sqrt{\frac{B\sigma_i}{\tau}} h_i W_i$$

in which B is a dimensionless coefficient between 0.3 and 1.5. Comparing [10] with the available data gives $B\sigma_i = 28$ kPa. If we use an "average" expression for l_i from Figure 9, then $B = 0.8$ and $\sigma_i = 34$ kPa which is in accord with what we would expect for the Thames River if we take the scale effect on strength into account (Appendix A).

VERTICAL BENDING

When runoff is increased, the ice cover will first crack longitudinally and eventually detach from the river banks. Once this has occurred, the cover becomes subject to vertical bending due to the distorted shape of the water surface. The latter may exhibit a wave-like form that travels in the downstream direction. The wave could be the result of increasing runoff or ice jam release or a combination of these effects. With reference to Figure 10, the total upward pressure applied on the ice cover

can be shown to be equal to $\gamma\delta - \gamma w$ for the region where the water level is below the top of the ice cover ($x \geq 0$); and equal to $\gamma(1 - s_i)h_i$ where the top ice surface is submerged ($x < 0$). Therefore, for $x \geq 0$, the ice cover may be considered a beam subjected to a distributed load ($= \gamma\delta$) and supported by an elastic foundation of modulus equal to γ . For $x < 0$, the ice cover acts as a free beam subjected to the uniform load $\gamma(1 - s_i)h_i$. Because δ and l_0 (= length of ice cover submergence, see Figure 10) are time-dependent, w is also time-dependent, i.e., $w = w(x,t)$. It follows that the differential equation describing w should include a term proportional to the vertical ice acceleration, $\frac{\partial^2 w}{\partial t^2}$. Based on an order of magnitude analysis, Billfalk (1982b) argued that this term can be neglected, so that any instantaneous distribution of w is produced by the static loading $\gamma\delta(x)$ that prevails at the same time. This assumption is retained herein (see also Beltaos, 1985).

To obtain $\delta(x)$, the form of the water surface should, strictly speaking, be determined from fluid dynamic considerations. However, this is a very complex task and a first approximation is to use an assumed shape of the water surface profile. This problem was first considered by Billfalk (1982a) who used a linear water surface. Beltaos (1985) assumed a negative exponential shape and took into consideration the effect of partial submergence of the upstream end of the ice sheet. The mathematical analyses involved are straightforward but tedious,

thus, the details will not be reproduced herein. The physical implications are discussed next.

Both Billfalk's and Beltaos' results suggest that flood waves are capable of breaking an ice sheet by bending, provided the water surface slope is 5×10^{-3} or more. Such slopes are rather extreme and unlikely to be produced by runoff alone; they could, however, prevail for a brief time after the release of a major jam. In this case, a series of closely spaced (order of $50 h_j$) transverse cracks³ would form for a certain distance downstream, until the wave slope attenuates to below the value required for fracture.

It should be recognized, however, that major ice jam releases can be attended by greatly augmented flow velocities and shear stresses. Breaking mechanisms, other than wave-slope bending, may now become operative and fracture the ice cover even if the water surface slope is well below the critical value derived earlier. For example, Ferrick et al. (1986) reported ice breaking at slopes as low as 0.5×10^{-4} .

The flow velocity, following the release of a jam, is roughly given by the equation (after simplification of Henderson and Gerard's (1981) analysis):

³provided the water surface is horizontal in the lateral direction. This should be generally the case, but short-lived transverse gradients may be set-up, for example, downstream of islands or when a tributary surge enters the main river. Fractures in the ice cover would then form a more complex pattern than a mere succession of transverse cracks.

$$[11] \quad u_s \approx u_0 + 0.4 \epsilon \sqrt{g y_0}$$

in which y_0 , u_0 = pre-release water depth and flow velocity (average) downstream of the jam; and ϵ = relative backwater caused by the jam = $(y_J - y_0)/y_0$, with y_J = water depth upstream of the jam. Eq. 11 suggests that in large rivers where both ϵ and y_0 are relatively large, the surging water velocity, u_s , can be several times more than u_0 . For example, a typical large river case would be $u_0 = 0.7$ m/s, $\epsilon = 1.0$ and $y_0 = 5$ m. Then $u_s = 3.5$ m/s so that $u_s/u_0 = 5$. The flow shear stress applied on the cover would be augmented by a factor of 25. Mechanisms that are not ordinarily capable of breaking the ice cover may now become effective, e.g., shear, ride-up and ridge formation, or "cutting"⁴. Horizontal bending is also augmented and closer-spaced transverse cracks may form (see Eq. 10).

THE ONSET OF BREAKUP

We have so far discussed several processes by which large ice sheets and floes may form. This, however, does not

⁴Due to the downward force that develops at an ice edge by local separation and water spillage over the ice. Wedge-shaped blocks break off and are carried under the cover so that a lane appears to be "cut" in the cover near the locus of maximum flow velocities.

necessarily lead to the onset of breakup because the ice sheets could remain stationary if no further changes in the river conditions occur. On the other hand, once ice sheets are set in motion, they quickly break down into small blocks by impacts at channel banks or on other sheets. This breakdown leads to formation of ice jams, surges and eventual ice clearance. It is thus convenient and common to define the onset of breakup at a given site as the time when the local ice cover is set in motion. This definition does not apply, however, where the ice cover is destroyed in-place either due to extreme thermal deterioration or by an ice run. The latter process is also known as a "breaking front" and it results from ice jam releases.

Criteria for the onset of breakup, deriving from the above processes, are discussed next.

The Boundary Constraint

Where a river reach is covered by a series of separate ice sheets, a criterion can be formulated by requiring that the water surface width be large enough to allow some of the sheets to move past bends or other obstacles. This concept was proposed by Beltaos (1984a) and enabled development of a criterion for breakup, using dimensional analysis. Herein, this concept is quantified using Beltaos' (1984a) simple expression for the movement of a curved ice sheet past a straight section, i.e.:

$$[12] \quad \frac{W_B}{W_i} - 1 = \left(\frac{R}{W_i} - 0.5 \right) \left(1 - \cos \frac{\theta}{2} \right)$$

in which W_B = water surface width where breakup is initiated;
 R = radius of curvature of the centre-line of the ice sheet;
 W_i = width of the sheet; and $\theta = l_i/R$, with l_i = length of
the sheet. For the expected range of θ (0 to $\pi/2$), the quantity
 $1 - \cos \theta/2$ can be closely approximated by $\theta^2/8 = l_i^2/8R^2$.
With this result and recalling Eq. 10, it is possible to recast
Eq. 12 as:

$$[13] \quad \frac{W_B}{W_i} - 1 = C \frac{100h_i}{W_i}$$

in which the coefficient C is defined by

$$[14] \quad C = \frac{m-0.5}{m^2} \frac{B\sigma_i}{800\tau}$$

with $m = R/W_i$. At a given site, m and τ do not change greatly
from year to year while σ_i should do likewise, provided
breakup starts before appreciable internal melting of the ice
cover occurs (e.g., see Bulatov 1972; Prowse et al. 1988) and
results from runoff increase rather than from a surge. Then C
should be roughly constant which explains earlier data (Beltaos
1984a) indicating linear plots of W_B/W_i versus $100 h_i/W_i$
at two river sites (Thames River, Ontario and Nashwaak River,
New Brunswick). Data from additional sites have been analyzed

since, showing similar trends (Figure 11) while the attendant scatter can be partly explained by plotting C versus a thermal index (Figure 12). When thermal effects are limited, i.e., thermal index $\rightarrow 0$ ("premature" breakup), C is maximum, as is plausible. Table 2 summarizes values of C_0 (= maximum C) at six sites. Despite the wide range of hydro-climatic conditions represented in Table 2, C_0 is in the narrow range of 0.45 to 0.90. It is difficult to pursue this line of analysis toward full prediction of C_0 because it depends on such parameters as m and τ (see [14]) which require laborious data processing and field measurements.

A more practical approach is to consider how the above theory can be simplified to give relationships that involve easily measurable quantities and, thence, explain some of the past empirical findings. For example, water level is empirically known to provide a good index of the onset of breakup on many occasions. If the reach-averaged river cross-section is assumed trapezoidal, [13] reduces to

$$[15] \quad H_B - H_F = Kh_i$$

in which H_B = water level at which the breakup starts, i.e., the ice cover is set in motion; H_F = water level corresponding to a channel width equal to the width of the ice cover, normally taken as the level during the preceding freeze up. The dimensionless coefficient K is defined by:

$$[16] \quad K = n(50C - \frac{l_s}{h_i}) = n[\frac{(m-0.5)B\sigma_i}{16 \tau m^2} - \frac{l_s}{h_i}]$$

with n = average river bank slope; and l_s = hinge crack distance from the edge and can be approximately calculated using Figure 4. In Eq. [16], it has been assumed that the river is wide enough so that two hinge cracks will form near the sides. Equation [15] is in agreement with past empirical findings showing H_B to vary linearly with H_F and h_i (e.g., Shulyakovskiy 1963; Beltaos 1984b, 1987). Values of K_0 , corresponding to "premature" events, are also summarized in Table 2 and fall mostly in the narrow range of 2.2 to 3.5. The large Thames River coefficient (8.0) is due to low water surface slope and steep river banks (i.e., low τ and high n , see [16]).

In many applications, the actual value of h_i when breakup starts is unknown; only the maximum winter thickness, h_{i0} , can be estimated with some confidence. In terms of h_{i0} , [15] can be rewritten as:

$$[17] \quad K_0 h_{i0} - (H_B - H_F) = K_1 \left[\frac{\sigma_i}{\sigma_{i0}} \Delta h_i + \left(1 - \frac{\sigma_i}{\sigma_{i0}}\right) h_{i0} \right]$$

in which σ_{i0} = undeteriorated flexural strength of the ice cover; $K_1 = 50 n C_0$ so that both K_1 and K_0 may be considered

site-specific constants; and Δh_i = reduction in ice thickness due to thermal inputs = $h_{i0} - h_i$. Ice strength reduction begins when penetrating solar radiation finds ice layers at 0°C and causes "candling", that is, melt around the crystal boundaries (Bulatov 1972; Ashton 1983). Therefore, the decay of the ice cover would initially consist of ice thickness reduction without appreciable loss of strength. The LHS of [17] would then vary in proportion to Δh_i which suggests that plotting $K_0 h_{i0} - (H_B - H_F)$ versus a thermal index would result in good correlations. Figure 13 shows such a relationship where, despite the scatter, the expected trend is confirmed. Similar results have been obtained for other sites (see for example, Beltaos 1984b and Tang *et al.* 1986).

Once the thermal effect is large enough to cause significant strength loss, this approach will produce increasing scatter, mainly because h_{i0} changes from year to year (see [17]). It should also be noted that the geometric constraint criterion could be rendered meaningless, if the thermal effect is so severe as to cause the cover to disintegrate before it moves. It follows that the present criterion would be easiest to apply in smaller streams and moderate latitudes where winter thaws are common and breakup is usually brought about before thermal deterioration becomes a serious factor.

Clearly, it would be desirable to devise numerical algorithms to compute, H_B , Δh_i and σ_i/σ_{i0} as functions of time via detailed analysis of flow, heat transfer and radiation absorption processes. Progress in this direction was made recently by Andres (1988) who developed a method to calculate ice thinning and open water area and applied it to the Athabasca River with good results. Prowse et al. (1988) obtained field data on ice strength decay and found a good relationship between the relative strength and the accumulated short-wave radiation adsorbed by the ice sheet, in accordance with previous theories and data.

The Breaking Front

The geometric constraint discussed in the previous section describes how breakup starts in cases of fairly competent ice cover and before major jams have formed. This type of initial ice movement, however, may not occur at all, if the ice cover is subjected to surges caused by the release of upstream jams. As already pointed out, the ice cover could then fracture in various ways owing to the surge-augmented hydrodynamic forces. In such instances, a "breaking front" often forms, i.e., a moving abrupt transition between the rubble from the released jam and the still intact sheet ice downstream. Breaking fronts have been observed to advance very rapidly and for long

distances before they come to a prolonged halt, thus forming a new jam. In this manner, a breaking front can efficiently reduce to rubble long sections of sheet ice cover (rates of advance of 5 m/s are not uncommon, for distances in the hundreds of kilometres; Gerard et al. 1984; Prowse 1986). The mechanisms by which the ice cover is broken up, however, are not known, perhaps because of the difficulties in making detailed and quantitative observations of so dynamic a phenomenon. The following descriptions provide qualitative insight.

Parkinson (1982) observed that surge arrival on the Liard-Mackenzie system was marked by a quick water level rise. The ice cover readjusted its shore contacts and hinges and slowly advanced 10-100 m until it wedged against the shores. This movement was attended by widespread breakage, with crack lines and crushed ice ridges spaced 10-50 m apart⁵. Following passage of the wave, the water level dropped and the now fractured cover remained stationary. Eventually the ice cleared after being lifted to a sufficiently high level by the rising discharge. Though a breaking front did not form in this case, Parkinson's (1982) observations elucidate one mechanism by which the surge wave, travelling faster than and well ahead of the rubble from the released jam, can cause fracture into small blocks.

⁵This is most likely caused by tensile stresses that develop some distance away from the impact point, see also Sanderson (1988).

Ferrick et al. (1986) identified two contrasting surge breakup behaviours, "high" and "low" energy breakups, based on their field experiments and observations. The "low" energy breakup is essentially what was earlier termed "cutting" and is likely to occur with thin covers. With "high" energy surges, "the entire ice sheet is forced downstream, breaking as necessary". The celerity of this type of fracture, resulting in large ice plates, approaches that of the surge. The ice plates were in motion though at a relatively low speed, while the breaking front advanced at an intermediate rate. The writer (unpublished) observed similar phenomena on the Restigouche River, N.B., during the 1988 breakup. There, however, the formation of ice plates ceased at some distance downstream of the original jam, and a new jam formed shortly after. The movement of the ice plates was attended by frequent ridges, particularly near the banks. It should be remembered, however, that the presence of moving ice plates ahead of the breaking front is not universal, e.g., see Prowse (1986).

Breaking fronts appear to be much slower in smaller rivers. The writer followed such a front for a few kilometers in the lower Thames River, Ontario (width \approx 100 m), thanks to access provided by local dykes. The front was V-shaped, pointing downstream, and moved at a rate of about 1.1 m/s. The front's motion was not continuous but it frequently halted for short time intervals, not exceeding a few minutes. Typically, the V-shaped front would "plow" through stationary sheet ice for

a few minutes before stopping. It appears that the rubble stoppage resulted in rising of the water level upstream until some "critical" condition was attained and movement resumed. Then the sheet ice ahead of the front and the rubble behind it moved together as if interlocked and only when the sheet ice began to slow down again, did the "plowing" action resume. Transverse cracks were noticed occasionally downstream of the front and secondary fronts developed where moving sheet ice encountered stationary one. Typically, the impact was followed by ride-ups and ridge formation. Puncture holes were also seen to form in the ice downstream of the fronts, with rubble emerging from underneath.

There are two major questions pertaining to breaking fronts: how fast they advance and under what conditions they are arrested to form new jams. No satisfactory answers exist at present, owing to the scarcity of detailed observational data. Important processes take place under the water and cannot be observed in the field. The laboratory is more suitable in this regard, but very little has been done toward simulating the ice cover breaking processes (e.g., see Wong et al. 1988). Before closing, we may note that the breaking speed u_f seems to be close to the surging water speed, u_s , resulting from a jam release (see [11]). For the Liard River in 1983 (Prowse, 1986), it is estimated that $\epsilon = 1.8$, $y_0 = 4$ m and $u_0 = 0.8$ m/s.

Then, from [11], $u_s = 5.3$ m/s which is close to the observed value of $u_f (= 5$ m/s). For the much smaller Thames River (1985) it is estimated that $\epsilon = 0.2$, $y_0 = 0.5$ and $u_0 = 0.9$ m/s. Then $u_s = 1.4$ m/s, close to the observed u_f of 1.1 m/s (note that u_f is an average rate of advance of the front and includes brief stoppages). It appears that the retarding force applied to the front by the breaking ice cover is small relative to the inertia of the rubble behind the front. This hypothesis is supported by order-of-magnitude estimates that can be obtained from ice mechanics literature (see, for example Sanderson 1988).

SUMMARY

The preceding discussion has examined some of the patterns and mechanisms by which an ice cover is likely to be fractured before it is set in motion, with applications to the onset of breakup. Emphasis has been on processes that are likely to occur when the ice cover retains a certain amount of integrity, i.e., it has not deteriorated thermally to the point of candling.

The first occurrence of fracture appears soon after the discharge begins to increase and is manifested by the formation of longitudinal cracks that, in streams of ordinary widths, are parallel and close to the banks. However, as the channel width decreases, the two cracks shift towards the centre and

eventually merge into a single, mid-channel crack. The relative location of the longitudinal or "hinge" cracks, l_s/W , is governed by the parameter λW , i.e., it depends on channel width as well as ice thickness, density and modulus of elasticity. In the case of a single crack, continuing rise in the water level is likely to lift the free ice edges at midstream and submerge the two ice strips if the far edges remain attached to the river banks. Eventually, heat transfer will cause detachment and free flotation of the side strips.

In the more usual case where two hinge cracks form, the middle portion of the ice cover will rise with the water level and eventually lose any support that might have been provided at points of contact with the side strips. At this time, the ice cover is still unable to move but is subject to relatively large stresses owing to loss of boundary support. In turn, these stresses lead to formation of transverse cracks.

Two mechanisms of transverse crack formation have been considered. The first mechanism involves bending on vertical planes due to an advancing water wave that tends to lift and deform the ice cover. Analysis indicates that crack spacing would be of the order of tens of ice thicknesses but extremely steep waves would be necessary to cause fracture. Such waves may occur briefly after the release of a major ice jam but the ice cover could then be destroyed by other processes via augmented hydrodynamic forces. Observed transverse crack

spacings of the order of a thousand ice thicknesses can be explained by horizontal bending which essentially arises from the meandering planform of natural streams.

The ice cover is thus reduced to a sequence of separate sheets which can be set in motion if there is enough room on the water surface. This is one way by which breakup can start and the associated criterion, herein called the boundary constraint, explains past empirical findings and identifies the factors influencing various empirical coefficients.

Another type of breakup initiation is caused by ice-jam release surges and the formation of breaking fronts whereby the ice cover is reduced to rubble before moving. Little is known about the details of motion of the breaking front. The rate of advance appears comparable to the surge velocity of the water following ice jam release.

REFERENCES

Anderson, J.C. 1982. Liard and Mackenzie River Ice Breakup, Fort Simpson Region, NWT, 1982. National Hydrology Research Institute Report, Ottawa (presently at Saskatoon).

Andres, D.D. 1988. Breakup Prediction in a Non-Regulated River. Proc. Workshop on Hydraulics of River Ice/Ice Jams, Winnipeg (in press).

Ashton, G.D. 1983. First Generation Model of Ice Deterioration. Proceedings of Conference on Frontiers in Hydraulic Engineering, ASCE, Cambridge, Mass., pp. 273-278.

Beltaos, S. 1983. Guidelines for Extraction of Ice-Breakup Data from Hydrometric Station Records. Draft Report Submitted to NRCC Working Groups on Ice Jams.

Beltaos, S. 1984a. A Conceptual Model of River Ice Breakup. Canadian Journal of Civil Engineering, Vol. 1, No. 3, pp. 516-529.

Beltaos, S. 1984b. Study of River Ice Breakup Using Hydrometric Station Records. Proc. Workshop on Hydraulics of River Ice, Fredericton, N.B., pp. 41-59.

Beltaos, S. 1985. Initial Fracture Patterns of River Ice Cover. NWRI Contribution #85-139, National Water Research Institute, Burlington, Ontario.

Beltaos, S. 1987. Ice Freeze Up and Breakup in the Lower Thames River: 1983-84 Observations. NWRI Contribution #87-19, National Water Research Institute, Burlington, Ontario.

Billfalk, L. 1981. Formation of Shore Cracks in Ice Covers due to Changes in the Water Level. Proceedings, IAHR International Symposium on Ice, Quebec, Canada, Vol. II, pp. 650-660.

Billfalk, L. 1982a. Breakup of Solid Ice Covers due to Rapid Water Level Variations. U.S. Army CRREL Report 82-3, Hanover, N.H.

Billfalk, L. 1982. Breakup of Solid Ice Covers due to Rapid Water Level Variations - A Note on Dynamic Effects. Swedish State Power Board, Technical Note, Alvkarleby, Sweden, 6 p.

Bulatov, S.N. 1972. Computation of the Strength of the Melting Ice Cover of Rivers and Reservoirs and Forecasting of the Time of its Erosion. Proceedings, IAHS Symposium on the Role of Snow and Ice in Hydrology, Vol. I, Banff, IAHS-AISH Publication No. 107, pp. 575-581.

Butyagin, I.P. 1972. Strength of Ice and Ice Cover (Nature Research on the Rivers of Siberia), U.S. Army CRREL, Draft Translation 327, Hanover, N.H.

Ferrick, M., Lemieux, G., Mulherin, N. and Demont, W. 1986. Controlled River Ice Breakup. Proceedings, IAHR Ice Symposium, Iowa City, USA, Vol. III, pp. 281-305.

Gerard, R., T.D. Kent, R. Janowicz, and R.O. Lyons. 1984. Ice Regime Reconnaissance, Yukon River, Yukon. Cold Regions Eng. Spec. Conf., Edmonton, Vol. III, pp. 1059-1073.

Gold, L.W. 1971. Use of Ice Covers for Transportation. Canadian Geotechnical Journal, 8, pp. 170-181.

Henderson, F.M. and R. Gerard. 1981. Flood Waves Caused by Ice Jam Formation and Failure. Proceedings, International Association for Hydraulic Research, International Symposium on Ice. Quebec, P.Q., pp. 277-297.

Hetenyi, M. 1946. Beams on Elastic Foundation. Ann Arbor: The University of Michigan Press.

KorzHAVIN, K.N. 1971. Action of Ice on Engineering Structures, U.S. Army CRREL AD 723 169, Hanover, N.H.

Nuttall, J.B. 1970. Observations on Breakup of River Ice in North Central Alberta. Canadian Geotechnical Journal, Vol. 7, pp. 457-463.

Parkinson, F.E. 1982. Water Temperature Observations During Breakup on the Liard-Mackenzie River System. Proceedings, Workshop on Hydraulics of Ice-Covered Rivers, Edmonton, Canada, pp. 261-290.

Prowse, T.D. 1986. Ice Jam Characteristics, Liard-Mackenzie Rivers Confluence. Canadian Journal of Civil Engineering, Vol. 13, No. 6, pp. 653-665.

Prowse, T.D. 1988. Using the Borehole Jack to Determine Changes in River Ice Strength. Proc. Workshop on Hydraulics of River Ice/Ice Jams (in press).

Sanderson, T.J.O. 1988. Ice Mechanics: Risks to Offshore Structures. Graham and Trotman. London/Dordrecht/Boston.

Shulyakovskii, L.G. (Editor). 1963. Manual of Forecasting Ice Formation for Rivers and Inland Lakes. Israel Program for Scientific Translations, Jerusalem, 1966.

Shulyakovskii, L.G. 1972. On a Model of the Breakup Process. Soviet Hydrology: Selected Papers, Issue No. 1, pp. 21-27.

Tang, P., Burrell, B., Lane, R., and Beltaos, S. 1986. Study of Ice Breakup in the Meduxnekeag River, N.B., Using Hydrometric Station Records. Proc., Fourth Workshop on Hydraulics of River Ice, Montreal.

Wong, J., Beltaos, S. and Moody, W. 1988. SYG-ICE: A Model Material for River Ice Breakup Studies. NWRI Contribution #88-86, National Water Research Institute, Burlington, Ontario.

Table 1. Characteristics of ice sheets observed in the Thames River (average values)

Date of Observation	Reach	h_1 (cm)	W_1 (m)	R (m)	l_1 (m)	α (m ²)	A (m ²)	Approx. τ (Pa)	Estimated σ_1 -Eq.9 (kPa)
Mar 17/82	Above Chatham; 30-40 km from river mouth	28	53	480	315	6,390	23,000 (est)	4.9	25-91
Feb 14/84	Above Chatham; 31-42 km from river mouth	30	57	542	307	6,640	23,950	5.8	27-97
Mar 16/84	Above Kent Bridge; 51-56 km from river mouth	10	43	415	159	1,170	6,690	3.4	11-63

Table 2. Values of coefficients C_0 and K_0 at six river sites

Site	Latitude (N)	Slope (m/km)	Long-term mean, open water		h_i (cm)	Average y_F^6 (m)	C_0	K_0
			Discharge (m^3/s)	Width (m)				
Thames River at Thamesville	42°32'42"	0.23	51	37	21	2.20	0.85	8.0
Ganaraska River near Dale	43°59'07"	1.80	3.4	17	29	0.55	0.90	3.5
Moose River at Moose River	50°48'50"	0.38	780	753	69	3.10	0.55	2.8
Nashwaak River at Durham Bridge	46°07'33"	0.73	36	58	60	2.10	0.45	2.5
Meduxnekeag River at Belleville ⁷	46°12'58"	1.80	26	48	51	1.65	0.65	3.1
Grand River near Marsville	43°51'43"	2.30	7.7	37	35	0.67	0.75	2.2

⁶Depth of flow under the ice cover, corresponding to the freeze up stage, H_f .

⁷Data source: Tang *et al.* (1986)

APPENDIX A

THE SCALE EFFECT ON THE HORIZONTAL BENDING OF ICE COVERS

It is well known by experience that the strength of ice specimens subjected to different loading configurations appears to decrease as the size of the specimen increases (e.g., see Butyagin 1972 and Sanderson 1988, who also discusses various theories that have been proposed to explain this finding). Butyagin's (1972) measurements on relatively small ice beams subjected to vertical bending indicated that the flexural strength, σ_1 , decreased with both beam width and beam thickness (= thickness of ice cover from which the beam was cut). Butyagin concluded that the strength reaches a finite limit once the beam width exceeds a value equal to seven ice thicknesses, but keeps on decreasing with increasing thickness, for the range tested ($h_1 \leq 1$ m). When the river ice cover is subjected to horizontal bending, its width is the dimension that corresponds to thickness in Butyagin's experiments. This dimension could thus amount to hundreds or thousands of metres.

To extend the range of Butyagin's results, a series of horizontal bending tests were performed in Rockwood Reservoir during January and February of 1988. The ice cover was about 33 cm thick and, to account for natural variations in ice strength, each large-scale test was accompanied by a small-scale

test on a 2.5 m long by 0.5 m wide cantilever. The large-scale tests were performed on cantilevers with a length-to-width ratio of 5 and with widths of 1 m, 2 m, 5 m, and 10 m.

Figure A.1 shows the results plotted in the form σ_i versus w = (beam width). A decreasing trend is evident but the scatter is considerable due to the large variation (200 - 750 kPa) in σ_{i0} (= strength of small beam; $w_0 = 0.5$ m). A much better trend is obtained by plotting relative strength, σ_i/σ_{i0} , versus w/w_0 as shown in Figure A.2 where corresponding data on vertical bending by Butyagin are also plotted for comparison. It is not possible to state whether σ_i decreases indefinitely or attains an asymptotic value at a certain width. We may note, however, that for $w = 10$ m, σ_i can be as low as 30 kPa (= 0.14 times lower limit of σ_0). If we use curve-fitting on the results of Figure A.2, we find

$$[A.1] \quad \frac{\sigma_i}{\sigma_{i0}} = \left(\frac{w}{w_0}\right)^{-0.6}$$

For the Thames River example discussed in the main text, the width of the ice cover is about 50 m. Then $w/w_0 = 100$ and $\sigma_i/\sigma_{i0} = 0.06$. For $\sigma_{i0} = 200 - 750$ kPa (Figure A.1) $\sigma_i = 13-47$ kPa which is comparable with the ranges estimated

in Table 1, deduced from the spacings of transverse cracks. Of course, this extrapolation is uncertain and only used to illustrate magnitudes rather than precise values.

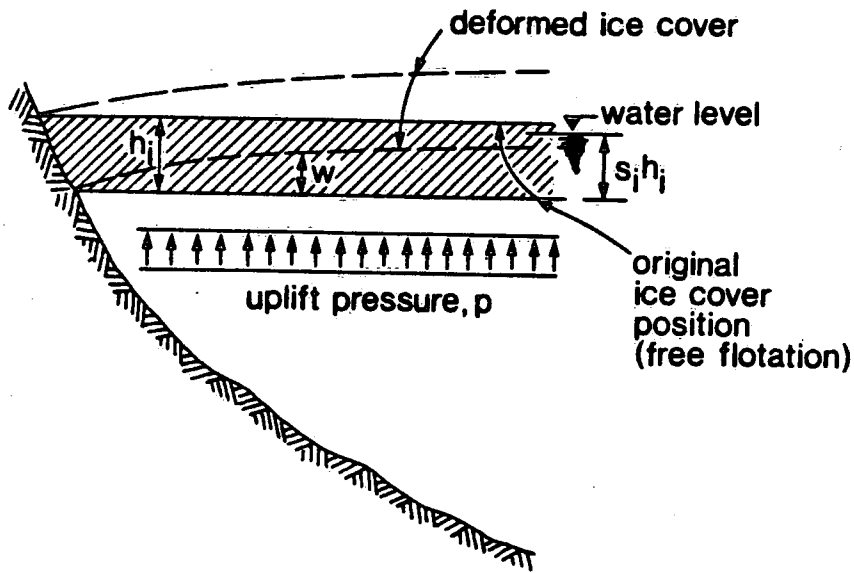


Fig. 1. River section with an ice cover, subjected to a distributed load P .

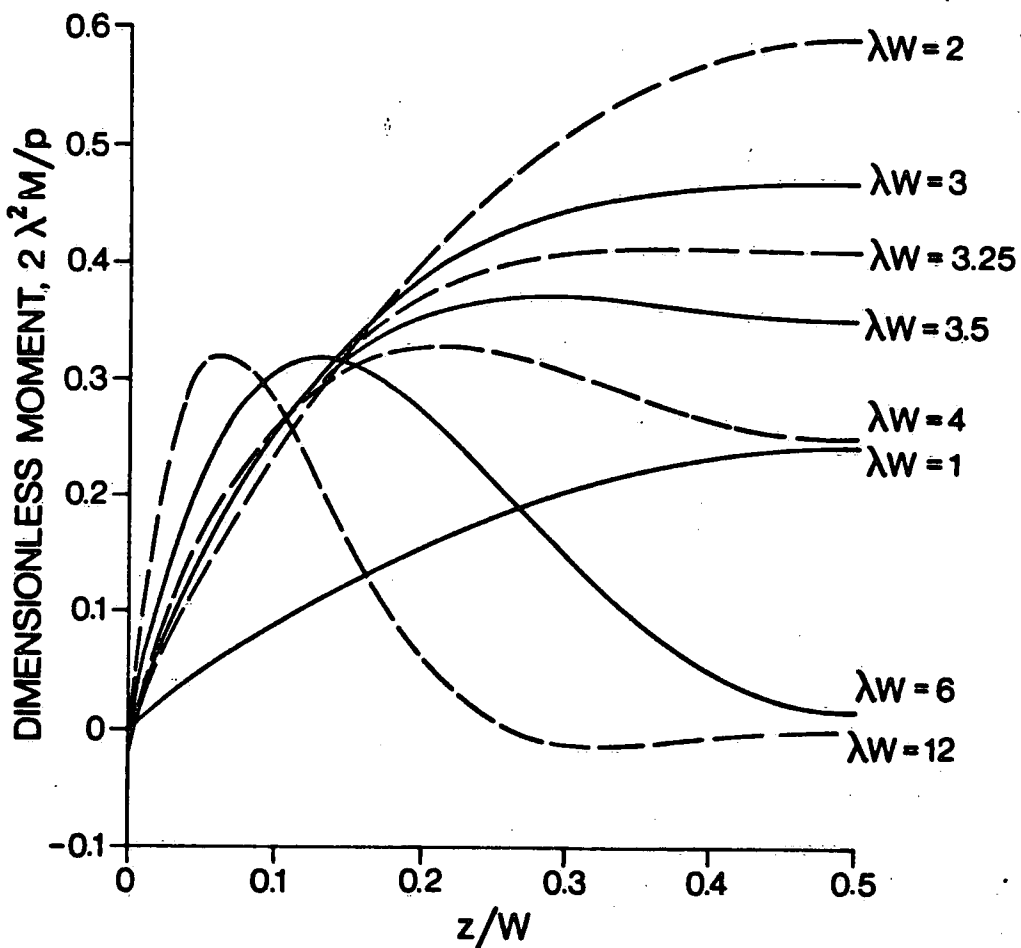


Fig. 2. Distribution of bending moment for hinged ends.

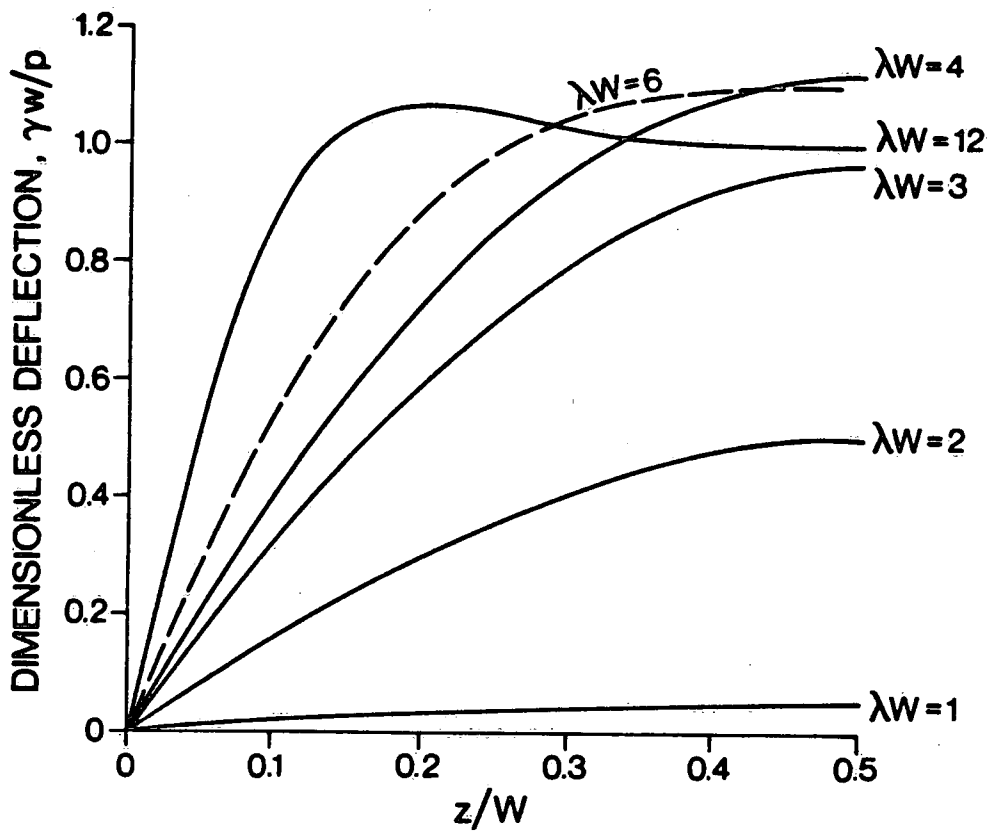


Fig. 3. Distribution of ice deflection for hinged ends.

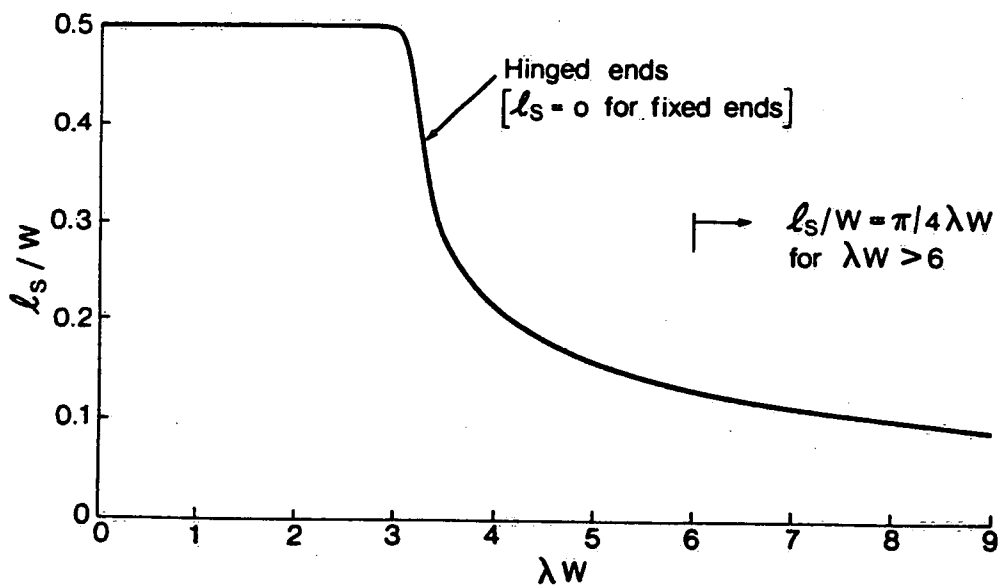


Fig. 4. Location of longitudinal cracks.

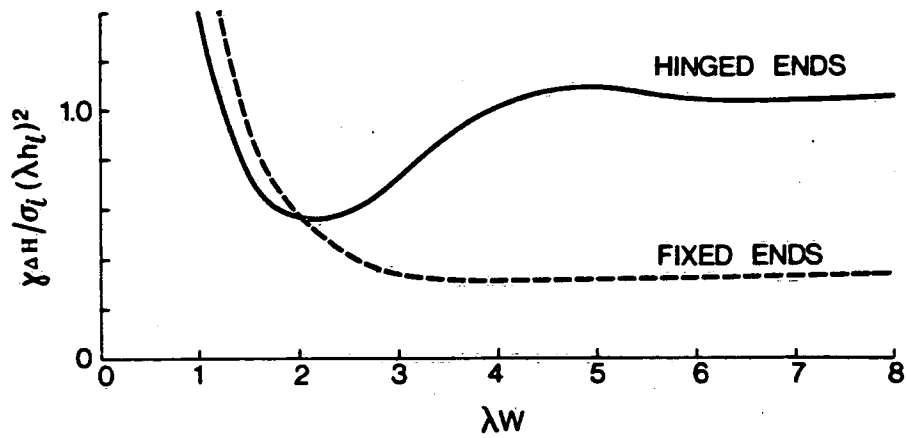


Fig. 5. Dimensionless uplift pressure required to cause longitudinal cracks.

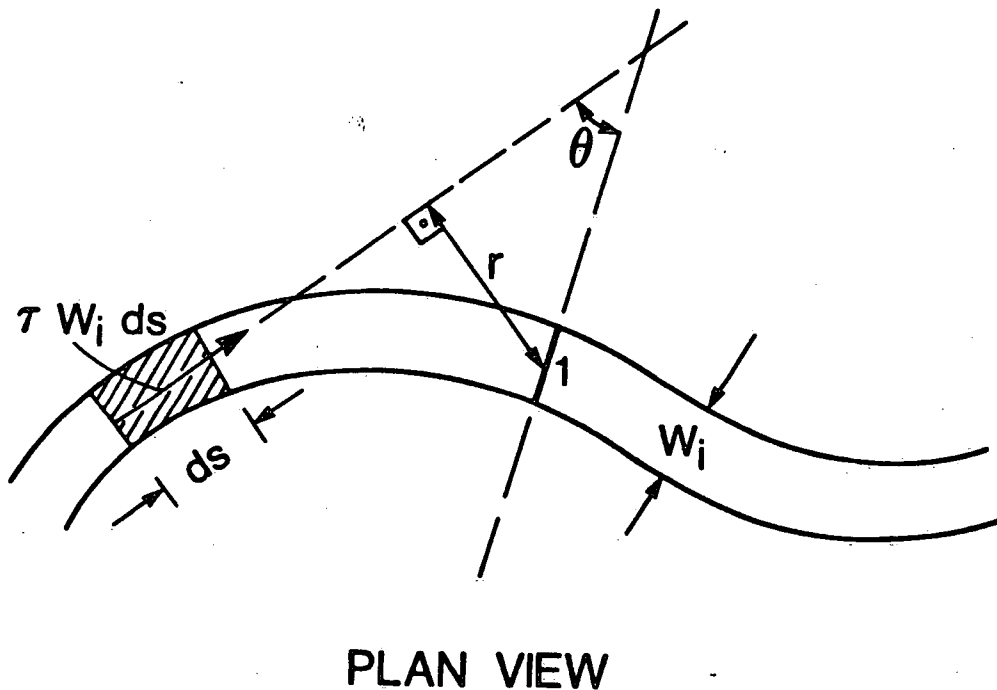


Fig. 6. Generation of stresses at section 1 due to tangential force τ : shear = $(\tau W_i ds) \cos \theta$; axial force = $(\tau W_i ds) \sin \theta$; bending moment = $(\tau W_i ds) r$.

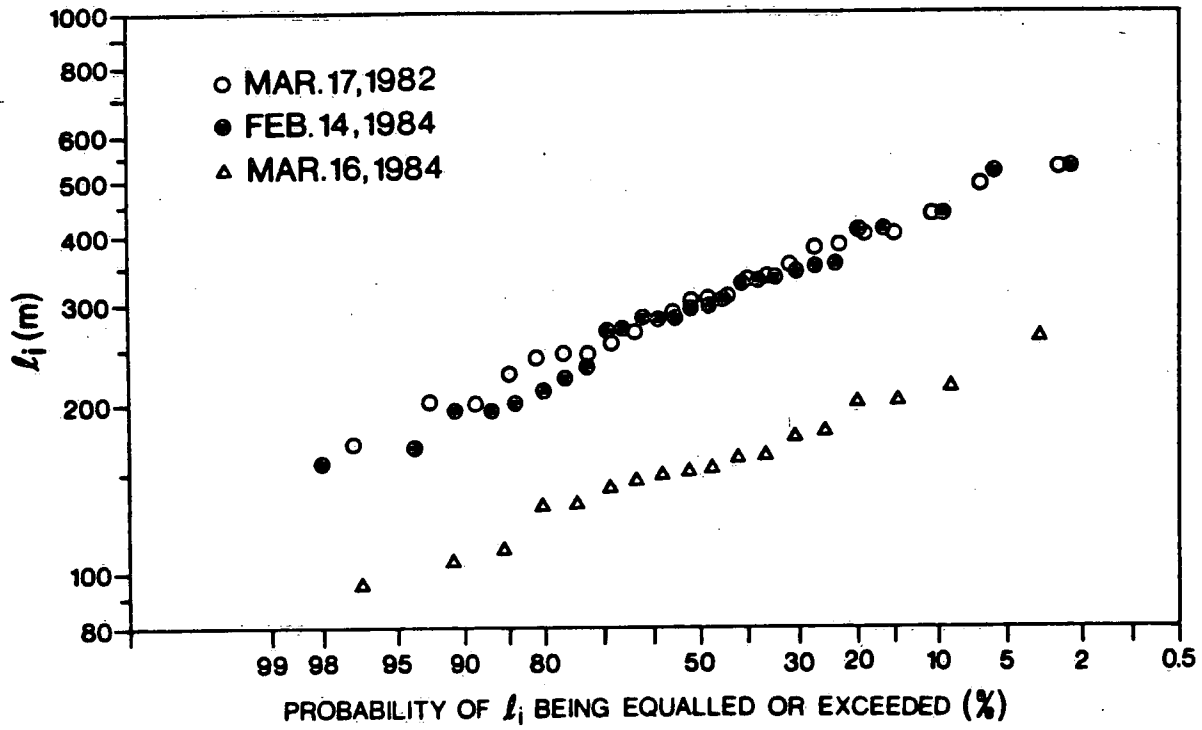


Fig. 7. Statistical distributions of lengths of ice sheets observed in the Thames River.

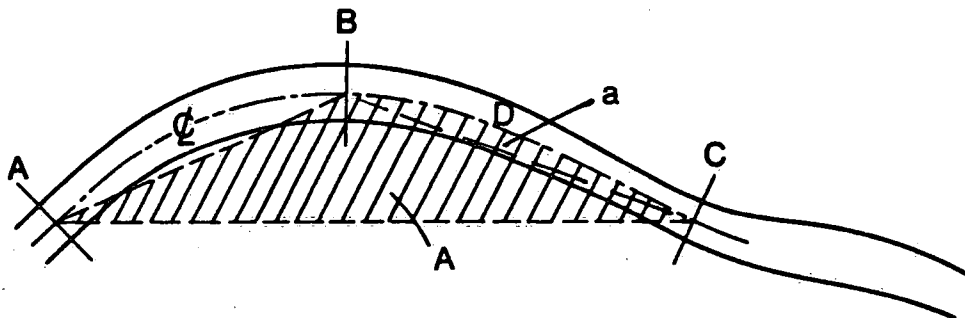


Fig. 8. Definition sketch for Equation (8); horizontal bending case. $A = (ABDCA)$; $a = (BDCB)$

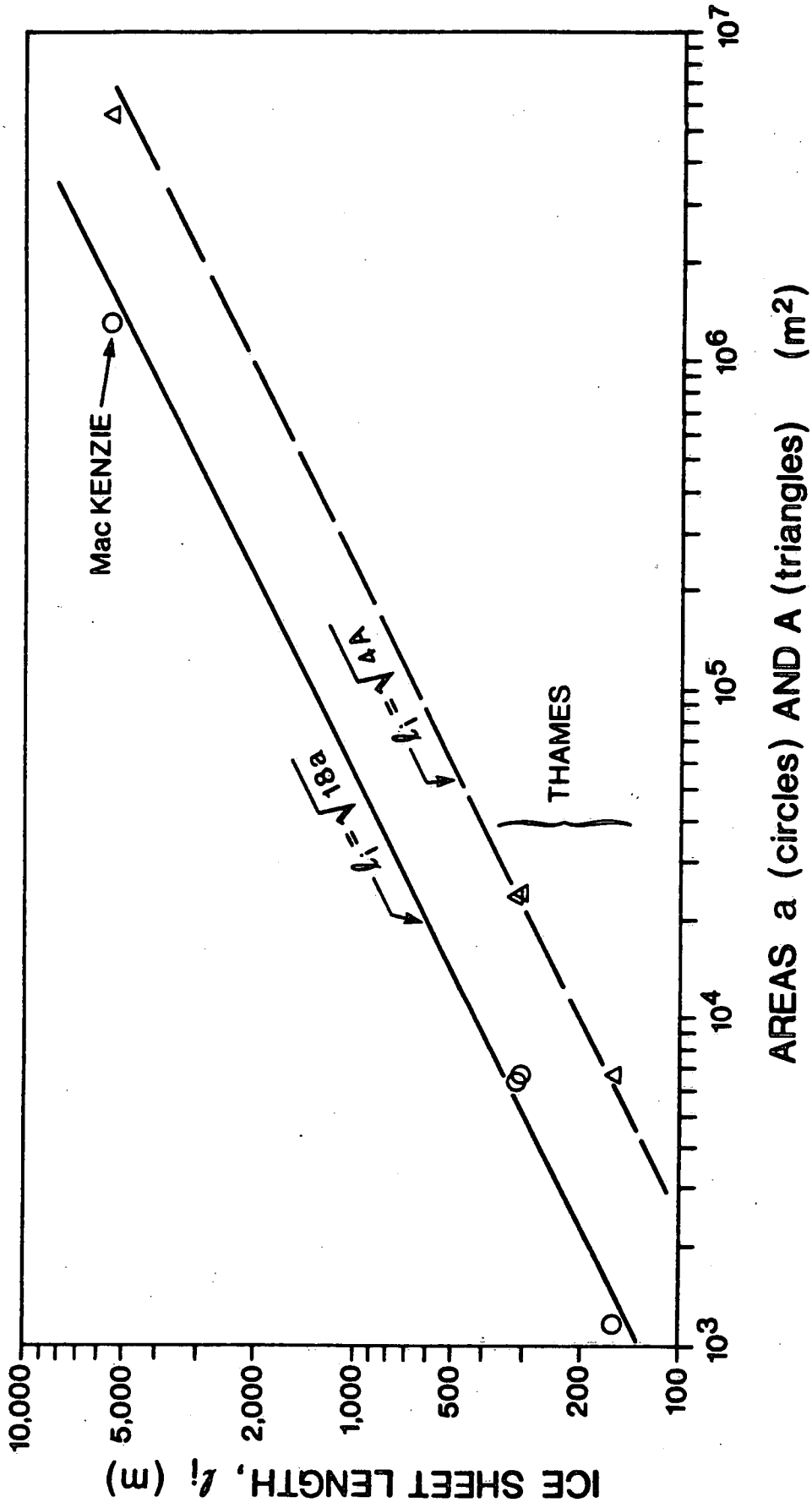


Fig. 9. Variation of ice sheet length with segment areas a and A .

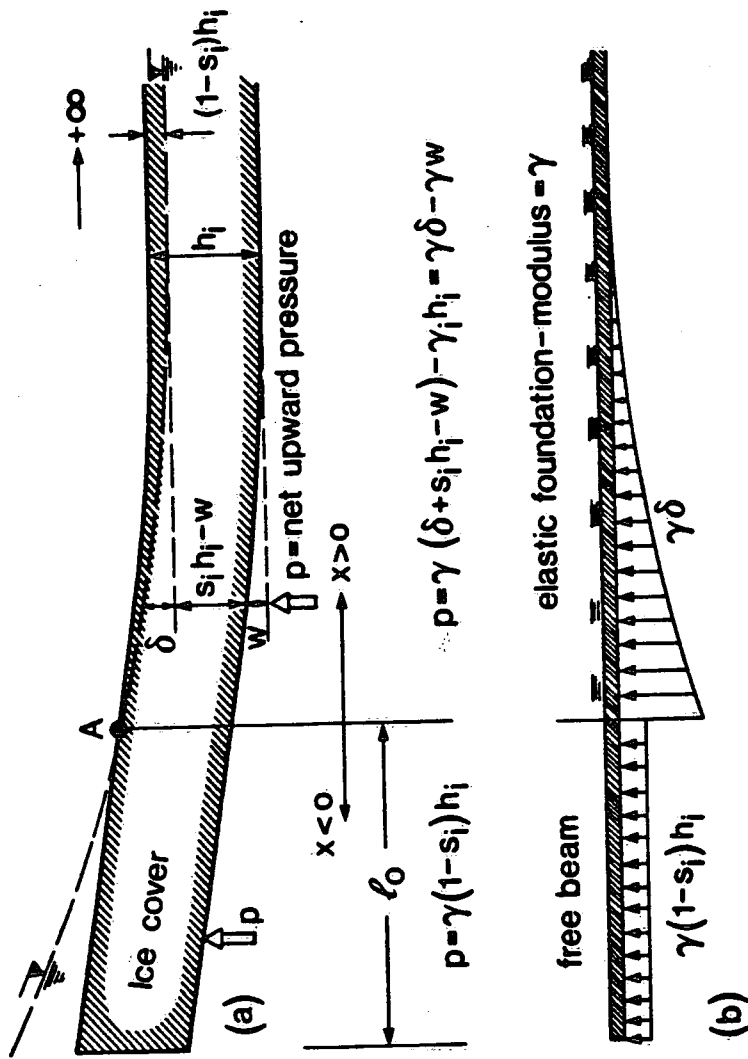


Fig. 10. Ice cover deformed by flood wave. (a) Definition sketch (b) Loading and support configurations

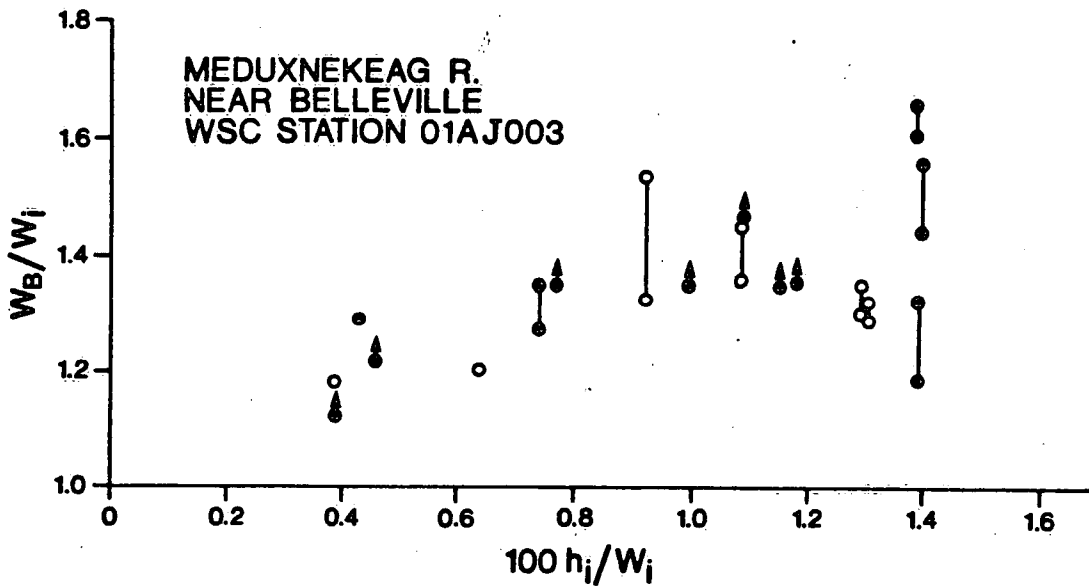
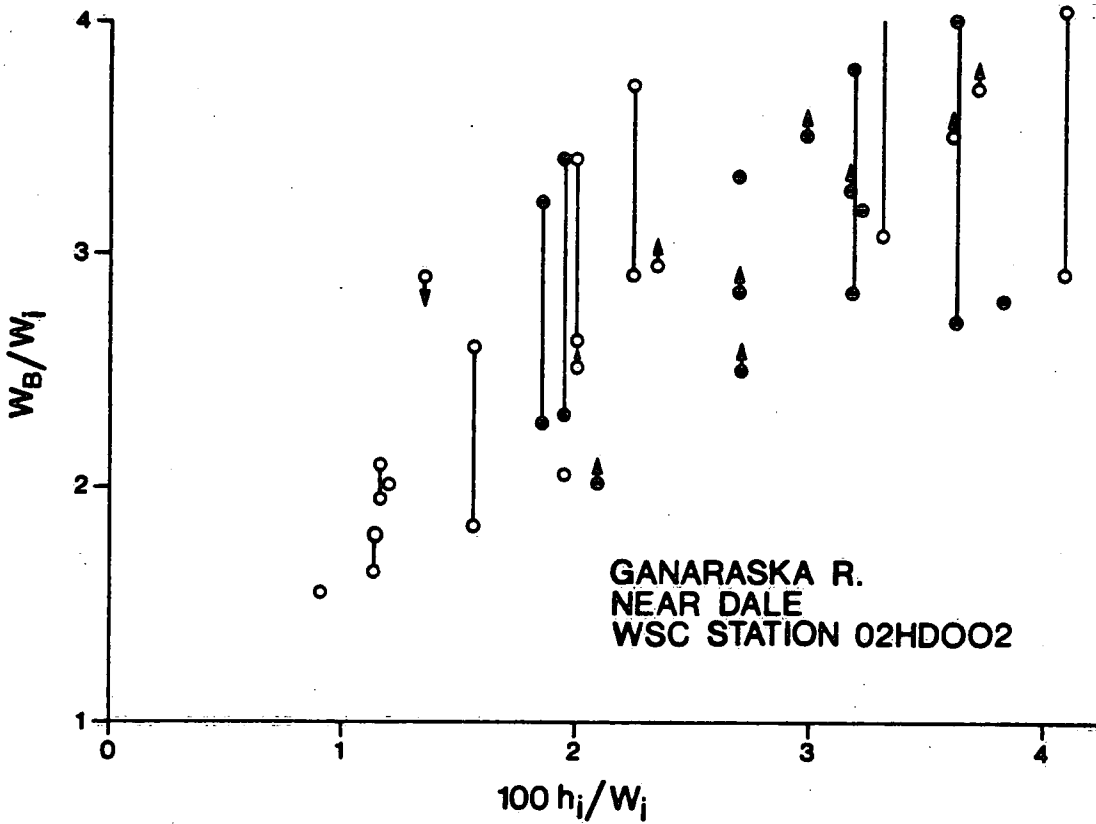


Fig. 11. Breakup initiation criteria at two river sites in Ontario (top) and New Brunswick (bottom), based on analysis of Water Survey of Canada records, as explained by Beltaos (1983). Tang et al. (1986) is the source of the Meduxnekeag R. data. Solid circles indicate more reliable data than open ones. Arrows indicate that a greater or lesser W_B would have been required to initiate breakup than the value corresponding to the data point located just above or below the arrow.

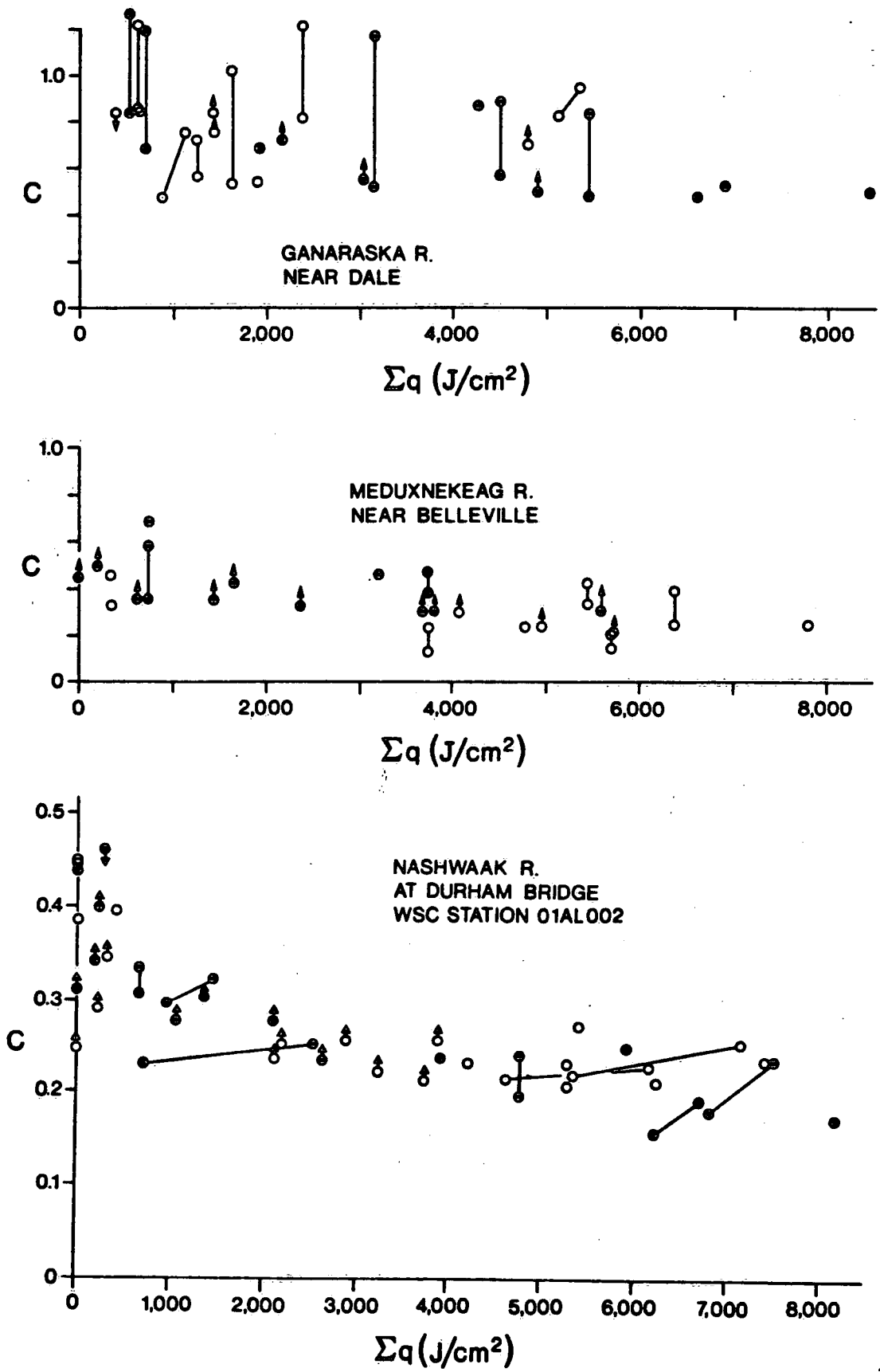


Fig. 12. Decline of coefficient C with cumulative thermal effects. Σq = index of accumulated heat transferred to the top surface of the ice cover prior to breakup, calculated according to Shulyakovsky (1963).

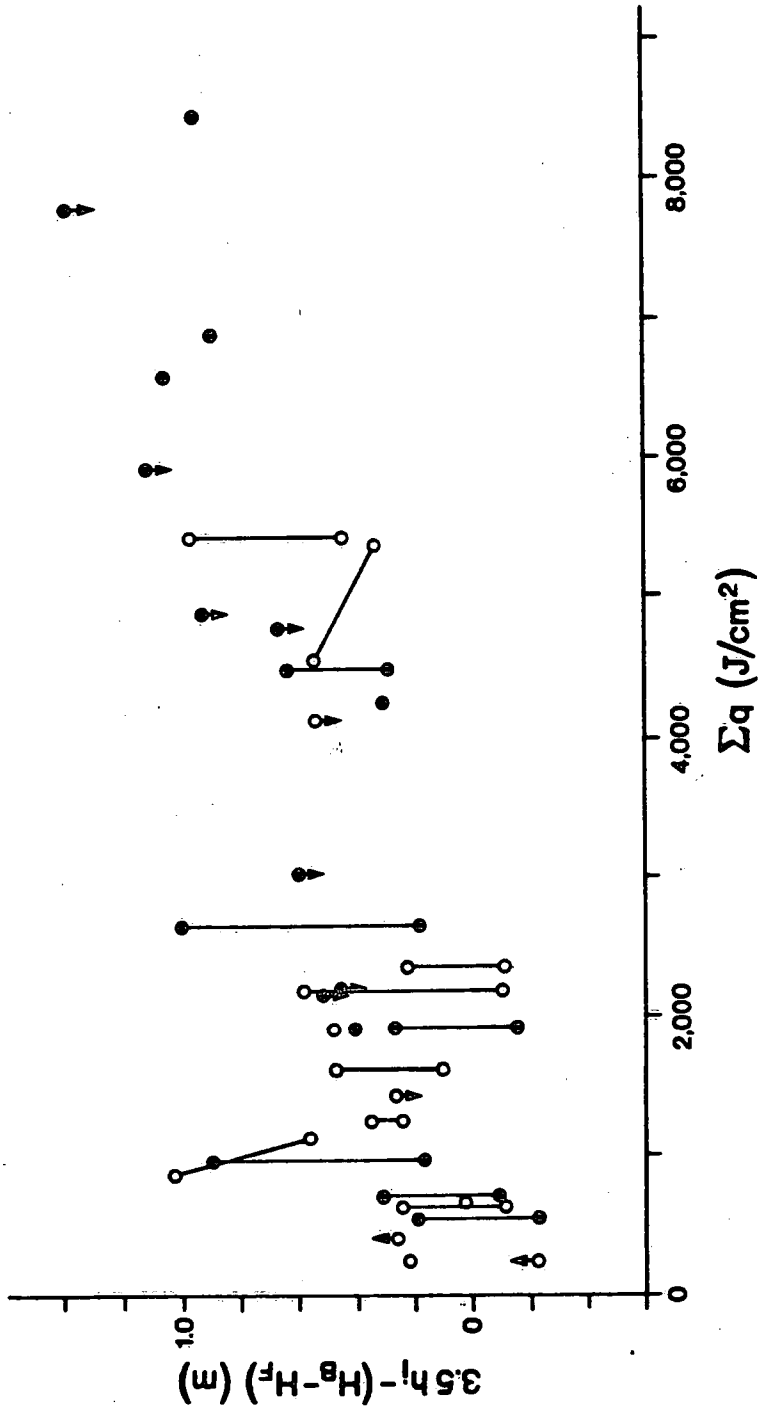


Fig. 13. Partial test of Equation 17 by plotting the LHS versus index of accumulated heat transfer to the ice cover. Ganaraska R. near Dale.

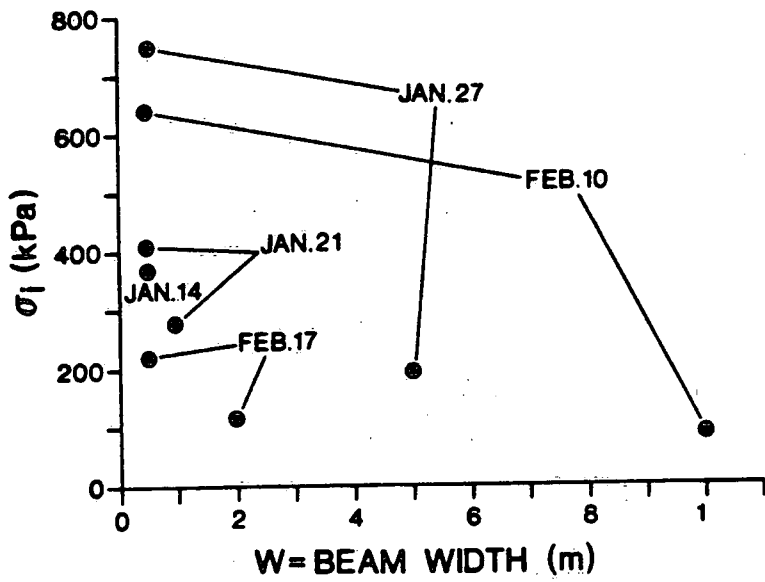


Fig. A.1. Flexural strength versus beam width.

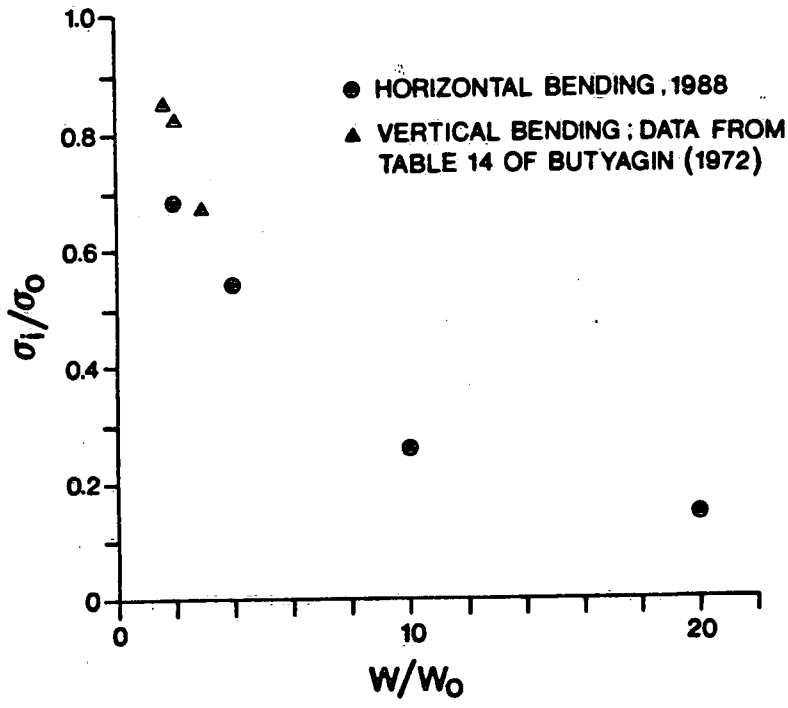


Fig. A.2. Relative flexural strength versus width ratio.